Original Article on Translational Imaging in Cancer Patient Care

# A pilot study on correlations between preoperative intravoxel incoherent motion MR imaging and postoperative histopathological features of rectal cancers

**Chenchen Yan[1*], Xia Pan[2*], Gang Chen[3], Wei Ge[3], Song Liu[2], Ming Li[2], Ling Nie[4], Jian He[1], Zhengyang Zhou[1]**

[1]Department of Radiology, Nanjing Drum Tower Hospital Clinical College of Nanjing Medical University, Nanjing 210008, China; [2]Department of Radiology, Drum Tower Hospital, Affiliated Hospital of Nanjing University Medical School, Nanjing 210008, China; [3]Department of Gastrointestinal Surgery, [4]Department of Pathology, Nanjing Drum Tower Hospital Clinical College of Nanjing Medical University, Nanjing 210008, China

*Contributions*: (I) Conception and design: C Yan, J He, Z Zhou; (II) Administrative support: J He, Z Zhou; (III) Provision of study materials or patients: G Chen, W Ge, L Nie; (IV) Collection and assembly of data: C Yan, X Pan, M Li; (V) Data analysis and interpretation: C Yan, X Pan, S Liu; (VI) Manuscript writing: All authors; (VII) Final approval of manuscript: All authors.

*These authors contributed equally to this work.

*Correspondence to:* Zhengyang Zhou, MD, PhD. Department of Radiology, Nanjing Drum Tower Hospital Clinical College of Nanjing Medical University, 321 Zhongshan Road, Nanjing 210008, China. Email: zyzhou@nju.edu.cn; Jian He, MD, PhD. Department of Radiology, Nanjing Drum Tower Hospital Clinical College of Nanjing Medical University, 321 Zhongshan Road, Nanjing 210008, China. Email: hjxueren@126.com.

**Background:** To explore the role of intravoxel incoherent motion (IVIM) magnetic resonance (MR) imaging in predicting the histopathological features of rectal cancers preoperatively.

**Methods:** Forty-six patients with a diagnosis of rectal cancer through endoscopic biopsy were prospectively enrolled and underwent IVIM MR imaging (12 b values: 0–1,200 s/mm$^2$) before surgery. Apparent diffusion coefficient (ADC), pure diffusion coefficient (D), perfusion-related incoherent microcirculation (D*) and perfusion fraction (f) values of the lesions were obtained and compared among rectal cancers with different histopathological features, including maximum diameter, pathological type, differentiation degree, TNM stage, lymphovascular and neural invasion status.

**Results:** The f and D* values of rectal cancers with lymphovascular invasion (LVI) were significantly higher than those without LVI (P=0.034, 0.037, respectively). And the LVI rate differed significantly among rectal cancers with different pN stages (P=0.003).

**Conclusions:** We demonstrated that the f value derived from IVIM MR imaging might be useful to predict LVI status of rectal cancers preoperatively, which required further confirmation in a larger cohort.

**Keywords:** Intravoxel incoherent motion (IVIM); magnetic resonance imaging (MR imaging); rectal cancers; histopathological features

Submitted Mar 03, 2017. Accepted for publication Aug 08, 2017.
doi: 10.21037/tcr.2017.08.23
**View this article at:** http://dx.doi.org/10.21037/tcr.2017.08.23

## Introduction

Nowadays, rectal cancer is an important contributor to cancer mortality and morbidity (1). It is well-known that histopathological features of rectal cancers play an important role in treatment optimization and prognosis prediction (2-4). However, most histopathological information could only be obtained from surgically resected specimens. Although endoscopic biopsy is routinely used to establish the diagnosis of rectal cancers in clinical practice, it is only restricted to the surface of the lesion with limited pathological information and unavoidable sampling error due to intratumoral heterogeneity (5).

Magnetic resonance (MR) imaging is currently widely used for preoperative staging in rectal carcinomas (6-9). Besides morphological MR imaging, functional sequences especially diffusion weighted (DW) imaging plays a more and more important role in evaluating microstructural characteristics noninvasively (10-13). For instance, correlations between pre-treatment apparent diffusion coefficient (ADC) values and several histopathological features of rectal cancers have been established by previous studies (14-16). However, the ADC value is affected not only by diffusion of water molecules, but also microcirculation in the capillary network (17), which caused some inconsistent results and confusion among those reports (14-16).

Based on the biexponential model developed by Le Bihan *et al.* (18), intravoxel incoherent motion (IVIM) MR imaging could distinguish fast diffusion (related mainly to micro-capillary perfusion) from slow diffusion (pure diffusion) (19). Pure diffusion coefficient (D), perfusion-related incoherent microcirculation (D*), as well as perfusion fraction (f) can be obtained through IVIM MR imaging (20,21). And the IVIM model has been successfully applied in characterizing the histopathological characteristics of liver (22,23), breast (24), pancreatic (25), renal (26), and prostate cancers (27,28).

Recently, IVIM MR imaging has been introduced into rectal cancer investigations, which mainly focused on therapeutic assessment and discrimination of lymph node metastasis (29-32). However, correlations between IVIM parameters and histopathological findings of rectal cancers have not been reported yet.

Thus, the aim of our study was to investigate the role of IVIM MR imaging in predicting the histopathological features of rectal cancers preoperatively.

## Methods

### *Patients*

This prospective study was approved by the local ethics committee at our hospital, and written informed consents were obtained from all the patients. The following inclusion criteria were employed: (I) all patients having preoperational pathological diagnosis of rectal cancer diagnosed by endoscopy-guided biopsy; (II) willing to receive MR examination for the purpose of preoperative evaluation; (III) without known allergies to intravenous contrast agents or other contraindications for MRI acquisition. The following exclusion criteria were employed: (I) with any prior anti-cancer therapy before treatment (n=27); (II) without postoperative pathological examination due to palliative operation or abandoned operation (n=5); (III) tumor with a minimum diameter less than 5 mm, which was not enough to cover a region of interest (ROI) for image analysis (n=6); (IV) poor image quality which was difficult to interpret (n=3).

From July 2015 to June 2016, of the 87 patients who met the inclusion criteria, additional 41 patients who met the exclusion criteria were eliminated. Finally, 46 patients (24 men, 22 women; mean age, 62.4±10.5 years; age range, 45–81 years) were included in this study (*Table 1*).

### *MR examination*

All patients fasted for 6–8 hours before MR examination to empty their gastrointestinal tracts. For reducing artifact caused by gas and feces within the enteric cavity, 139 g of polyethylene glycol electrolyte powder compound (139 g: 2,000 mL water; Jiangxi Hygecon Drug Research Institute Company Limited, Shangrao, China) was taken orally 5 hours before MR imaging for those patients who can eat laxatives (n=33), and clyster was taken 2 hours prior to MR examination for those patients with bowel obstruction (n=13).

All patients were scanned in a supine position with head first on a 3.0 T MR scanner (Ingenia, Philips Medical Systems, Best, the Netherlands) with a dStream Torso coil. The scan ranged from the superior border of ilium to lower margin of the pubic bone. The MR sequences with detailed acquisition parameters are summarized (*Table 2*). The IVIM sequence was based on standard single-shot DW spin echo planar imaging with 12 b values (0, 25, 50, 75, 100, 150, 200, 400, 600, 800, 1,000, and 1,200 s/mm$^2$). The total acquisition time was about 20 min. The mean interval

 

**Table 1** Clinicopathological features of patients with rectal carcinomas

| Parameters | Groups | n=46 | Percentage (%) |
|---|---|---|---|
| Age | ≥60 years | 29 | 63.0 |
| | <60 years | 17 | 37.0 |
| Gender | Male | 24 | 52.2 |
| | Female | 22 | 47.8 |
| Carcinoembryonic antigen | ≥5 ng/mL | 25 | 54.3 |
| | <5 ng/mL | 21 | 45.7 |
| Cancer antigen 19-9 | ≥37 μ/mL | 9 | 19.6 |
| | <37 μ/mL | 37 | 80.4 |
| Pathological type | Adenocarcinoma | 46 | 100 |
| | Mucinous adenocarcinoma | 0 | 0 |
| Differentiation degree | Poor | 1 | 2.2 |
| | Poor-moderate | 9 | 19.6 |
| | Moderate | 33 | 71.7 |
| | Moderate-well | 1 | 2.2 |
| | Well | 2 | 4.3 |
| pT | T1 | 3 | 6.5 |
| | T2 | 10 | 21.7 |
| | T3 | 33 | 71.7 |
| | T4 | 0 | 0 |
| pN | N0 | 20 | 43.5 |
| | N1 | 15 | 32.6 |
| | N2 | 11 | 23.9 |
| cM | M0 | 44 | 95.7 |
| | M1 | 2 | 4.3 |
| Overall stage | I | 9 | 19.6 |
| | II | 11 | 23.9 |
| | III | 24 | 52.2 |
| | IV | 2 | 4.3 |
| Lymphovascular invasion | Absent | 29 | 63.0 |
| | Present | 17 | 37.0 |
| Neural invasion | Absent | 21 | 45.7 |
| | Present | 25 | 54.3 |

between MR examination and surgery was 3.2±0.8 days (range, 1–6 days).

### *Image analyses*

IVIM parameter measurements were conducted by two independent readers (CCY, XP, with 6 and 2 years' experience in digestive radiology, respectively), who were blinded to the colonoscopic and surgical pathological results.

The IVIM data were evaluated using DWI-Tool developed by Philips (IDL 6.3, ITT Visual Information Solutions, Boulder, CO, USA) to generate ADC, D, f and D* maps, which used the robust nonlinear least-squares curve fittings based on the Levenberg-Marquardt algorithm. ADC value was obtained with 12 b values from mono-exponential fit to the equation: $S = S_0 \times \exp(-b \times ADC)$, Where $S_0$ represents the signal without diffusion weighting and S is the signal with diffusion weighting. And a bi-exponential model was applied to calculate D, f, and D* values with the following function described by Le Bihan *et al.* (19):

$$SI/SI_0 = (1-f) \times \exp(-b \times D) + f \times \exp(-b \times D^*) \quad [1]$$

in which SI is the signal intensity at a certain b value and $SI_0$ is the signal intensity at a b value of 0 s/mm$^2$. Because D* is roughly one order of magnitude greater than D (33), –bD* is less than –3 at a high b value (>200 s/mm$^2$) and f exp(–bD*) is less than 0.05f. In this case, the contribution of D* to the Sb/S0 signal ratio can be ignored, and Eq. [1] can be simplified to Eq. [2] to estimate D:

$$SI/SI0 = \exp(-b \times D) \quad [2]$$

Thus, for the high b values (larger than 200 s/mm$^2$), SI was first fitted to Eq. [2] with a linear model, and D was calculated. Then, the f and D* coefficients were computed using Eq. [1] for all b values considering the calculated D values by a nonlinear Levenberg-Marquardt method. Lemke *et al.* (34) demonstrated that overestimation of f was dependent on echo time. The longer the echo time, the greater the signal decays at low b values, which indicates the increase of estimated f. The echo time in our study was 59 ms, which was relatively shorter than those in the literatures (35,36) and benefit for f measurement.

On MR imaging, the rectal cancer presented as a mass

 

**Table 2** MR sequences performed on patients with rectal cancers

| Sequence | T2 weighted imaging | T2 weighted imaging | T2 weighted imaging | IVIM imaging | Contrast enhanced imaging |
|---|---|---|---|---|---|
| Plane | Sagittal | Axial | Coronal | Axial | Axial |
| Repetition time (ms) | 1,700–5,000 | 1,700–5,000 | 3,000 | 6,000 | 3.1 |
| Echo time (ms) | 100 | 100 | 75 | 59 | 1.48 |
| Section thickness (mm) | 4 | 4 | 3 | 4 | 1.5 |
| Intersection gap (mm) | 1 | 1 | 1 | 1 | 0 |
| Field of view (cm) | 24×24 | 24×15.9 | 18×12.7 | 30×15.9 | 38.2×29.2 |
| Acquisition matrix | 480×354 | 480×300 | 300×189 | 80×143 | 256×194 |
| Number of signals averaged | 2 | 2 | 2 | 2 | 1 |
| Acquisition time (min) | 3.36 | 3.41 | 5.42 | 6.54 | 0.13 |

IVIM, intravoxel incoherent motion.

with hyperintense on T2-weighted and IVIM images and isointense on T1-weighted images compared with normal rectum wall, with remarkable enhancement on contrast enhanced sequence. With the reference to other MR sequences, three axial IVIM images (b=1,000 s/mm$^2$) which displayed the largest area of the tumor were selected. The ROIs were manually drawn within the solid part of the lesion as large as possible (mean: 68.8±6.5 mm$^2$; range, 50.3–80.2 mm$^2$) carefully excluding necrotic and cystic areas and hemorrhage. The ROIs were automatically copied to the ADC, D, f and D* maps and the mean value of each ROI was recorded. Average value of those three slices and mean values of the two radiologists were calculated as the final results for statistical analyses (*Figures 1*,*2*).

### *Surgical pathological analysis*

Twenty-eight patients underwent Dixon surgery, while fourteen patients received Miles surgery, and four patients underwent Hartmann surgery. Each patient had one lesion identified. Histopathological analysis of the resected specimens was performed by the pathologist (LN, with 5 years' experience in gastrointestinal pathology). The maximum diameter of each cancer lesion was measured and recorded. Histopathological type, differentiation degree, lymphovascular and neural invasion were analyzed. Especially, the presence of lymphovascular invasion (LVI) was determined according to the following criteria: presence of tumor cells within a vascular space; erythrocytes surrounding the tumor cells; identification of endothelial cells lining the space; the presence of an elastic lamina surrounding tumor; and attachment of tumor cells to the vascular wall (37). Pathological stages of those tumors were documented according to the 7th American Joint Committee on Cancer TNM staging system.

### *Statistical analyses*

Quantitative values in normal distribution were recorded as the means ± standard deviations (SD). Those IVIM parameters of rectal carcinomas with different histopathological features were compared with independent-samples *t*-test or one-way analysis of variance followed by the post hoc Tukey's test. The IVIM parameters in non-normal distribution were compared with Mann-Whitney U test or Kruskal-Wallis test. For those analyses with significant findings, receiver operating characteristic curve (ROC) analysis as well as Chi-square test was further implemented. The inter-observer agreement of IVIM parameters measurement was assessed with intraclass correlation coefficient (ICC): poor (less than 0.400), fair (0.400–0.600), good (0.600–0.750), and excellent (0.750–1.000). Statistical analysis was performed with SPSS 18.0 software (SPSS Inc., Chicago, IL, USA). P values <0.05 were taken to indicate statistical significance in all cases.

## Results

The f and D* values of rectal cancers with LVI were significantly higher than those without LVI (P=0.034, 0.037, respectively) (*Table 3*). The f and D* values differentiated

 

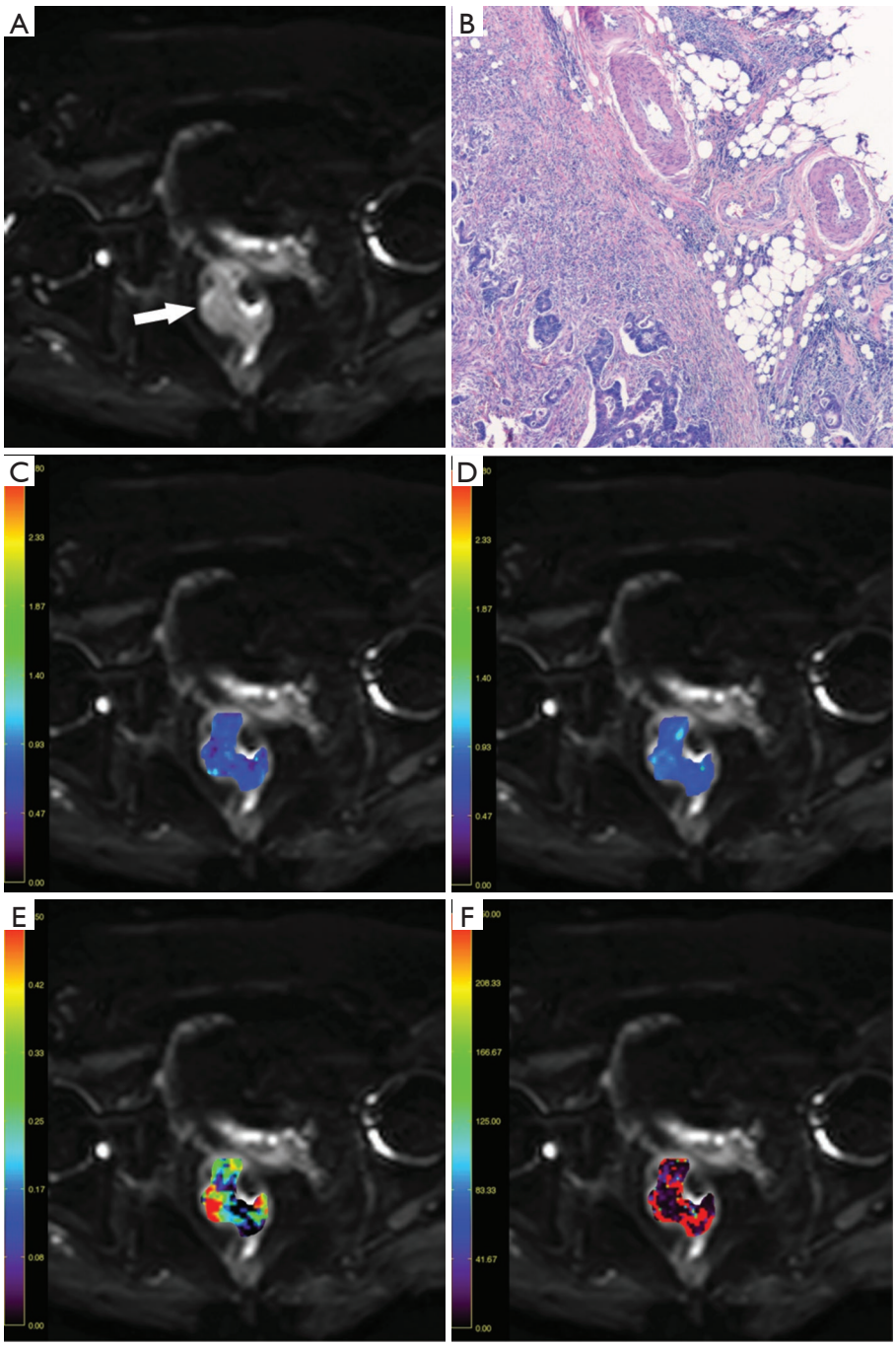


**Figure 1** A 67-year-old man with rectal cancer pathologically diagnosed at stage T3N0cM0. (A) Axial intravoxel incoherent motion (IVIM) magnetic resonance (MR) image (b=0 s/mm$^2$) shows a mass in the rectal wall (white arrow) with remarkably high signal intensity; (B) photomicrograph (Hematoxylin & Eosin staining, ×200) shows an adenocarcinoma without lymphovascular invasion; The corresponding (C) apparent diffusion coefficient (ADC), (D) pure diffusion coefficient D, (E) perfusion related fraction f; and (F) pseudo diffusion coefficient D* maps fused with (A) show that this lesion has an ADC value of $0.896\times10^{-3}$ mm$^2$/s, a D value of $0.799\times10^{-3}$ mm$^2$/s, a f value of 0.157 and a D* value of 23.417 mm$^2$/s, respectively.

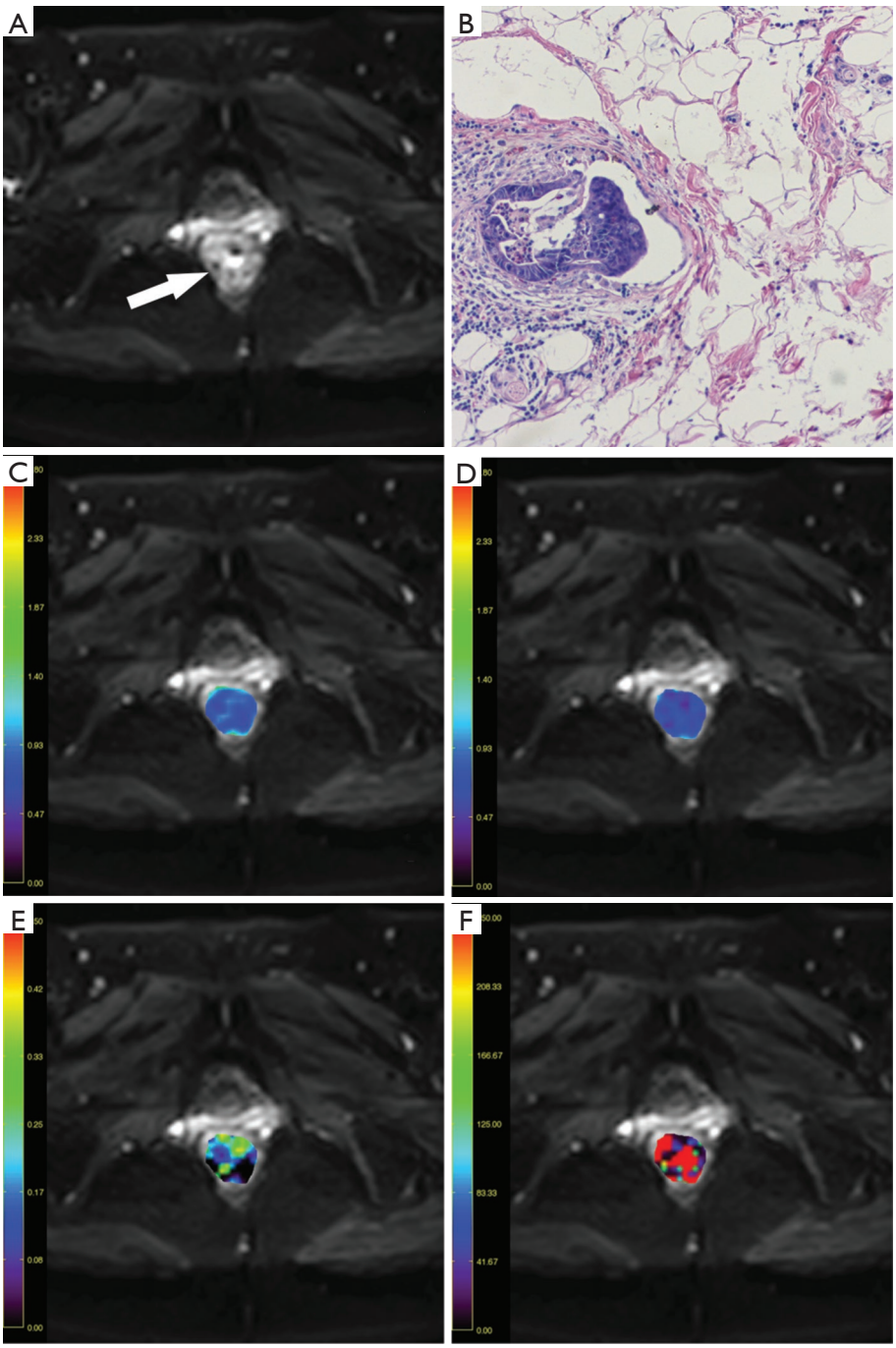


**Figure 2** A 65-year-old woman with rectal cancer pathologically diagnosed at stage T3N2bcM0. (A) Axial intravoxel incoherent motion (IVIM) magnetic resonance (MR) image (b=0 s/mm$^2$) shows a mass in the rectum (white arrow) with remarkably hyperintensity; (B) photomicrograph (Hematoxylin & Eosin staining, ×200) shows an adenocarcinoma with tumor cells invading into the lymphovascular structure; The corresponding (C) apparent diffusion coefficient (ADC), (D) pure diffusion coefficient D, (E) perfusion related fraction f; and (F) pseudo diffusion coefficient D* maps fused with (A) show that this lesion has an ADC value of $0.801\times10^{-3}$ mm$^2$/s, a D value of $0.731\times10^{-3}$ mm$^2$/s, a f value of 0.079 and a D* value of 25.208 mm$^2$/s, respectively.

 

**Table 3** Maximum diameter and intravoxel incoherent motion (IVIM) parameters of rectal carcinomas with different pathological features

| Parameters | Groups | Maximum diameter (cm) | ADC ($\times10^{-3}$ mm$^2$/s) | D ($\times10^{-3}$ mm$^2$/s) | f | D* ($\times10^{-3}$ mm$^2$/s) |
|---|---|---|---|---|---|---|
| Differentiation degree | P-M | 3.958±1.158 | 0.927±0.044 | 0.715±0.028 | 0.188±0.032 | 17.935±11.486 |
| | M-W | 4.190±0.884 | 0.912±0.053 | 0.723±0.032 | 0.174±0.039 | 25.468±21.299 |
| pT | T1 | 2.667±1.041 | 0.929±0.007 | 0.712±0.005 | 0.191±0.003 | 16.508±0.782 |
| | T2 | 3.200±0.943 | 0.945±0.075 | 0.713±0.049 | 0.201±0.048 | 16.429±8.494 |
| | T3 | 4.376±0.933 | 0.916±0.033 | 0.718±0.022 | 0.180±0.029 | 20.804±16.122 |
| pN | N0 | 3.765±1.127 | 0.931±0.035 | 0.718±0.027 | 0.189±0.011 | 15.225±3.190 |
| | N1 | 4.247±1.166 | 0.915±0.063 | 0.719±0.040 | 0.178±0.056 | 25.073±19.105 |
| | N2 | 4.127±0.951 | 0.922±0.035 | 0.711±0.007 | 0.188±0.020 | 19.977±17.343 |
| cM | M0 | 3.975±1.111 | 0.924±0.047 | 0.717±0.030 | 0.185±0.035 | 19.885±14.504 |
| | M1 | 4.750±0.354 | 0.914±0.010 | 0.710±0.011 | 0.186±0.001 | 12.706±0.341 |
| Overall stage | I | 3.033±1.002 | 0.945±0.041 | 0.725±0.039 | 0.192±0.012 | 13.743±3.042 |
| | II | 4.364±0.856 | 0.919±0.025 | 0.712±0.007 | 0.186±0.009 | 16.438±2.887 |
| | III | 4.150±1.091 | 0.918±0.054 | 0.716±0.032 | 0.182±0.046 | 23.768±18.716 |
| | IV | 4.750±0.354 | 0.914±0.010 | 0.710±0.011 | 0.186±0.001 | 12.706±0.341 |
| Lymphovascular invasion | Absent | 3.876±1.134 | 0.916±0.071 | 0.720±0.067 | 0.177±0.009 | 21.976±9.248 |
| | Present | 4.235±1.030 | 0.936±0.108 | 0.710±0.046 | 0.199±0.101* | 15.050±0.586* |
| Neural invasion | Absent | 3.952±1.136 | 0.915±0.034 | 0.710±0.038 | 0.185±0.008 | 19.344±11.700 |
| | Present | 4.056±1.089 | 0.930±0.088 | 0.722±0.103 | 0.185±0.127 | 19.582±13.525 |

*, P<0.05 (two independent samples *t*-test). ADC, apparent diffusion coefficient; D, pure diffusion coefficient; f, perfusion fraction; D*, pseudo-diffusion coefficient; P-M, poor + poor-moderate; M-W, moderate + moderate-well + well.

rectal cancers with and without LVI with AUC of 0.629 and 0.647, yet with P values of 0.148 and 0.099, respectively. LVI rate differed significantly among rectal cancers with different pN stages (P=0.003). Measurements of IVIM parameters in rectal cancers showed good inter-observers agreement (ICC, 0.615–0.713).

## Discussion

The present study revealed the feasibility of IVIM imaging for preoperative evaluation of rectal cancers. Correlations between IVIM parameters and histopathological features of rectal cancers were comprehensively investigated in our study and some interesting findings were obtained.

LVI, which was characterized by the extension of tumor cells into lymphatic and/or blood vessels, has been widely accepted as an independent prognostic factor, and a good indicator of adjuvant therapy in colorectal cancers. We found that rectal cancers with LVI showed higher f values compared with those without LVI. Since f value corresponded to the vascular volume fraction of the tumor, we speculated that tumors with abundant blood supply tended to involve with LVI. It was in accordance with the published reports. Wu *et al.* (38) found that the diameter of superior hemorrhoidal vein was significantly larger in rectal cancers with LVI than those without, probably due to increased venous drainage because of tumor hypervascularity. Yao *et al.* (39) showed a significant difference of $K_{trans}$ value derived from dynamic contrast-enhanced MR imaging between rectal cancers with and without lymphatic involvement. Moreover, an increased D* value was also detected in rectal cancers with LVI. The perfusion related fast diffusion coefficient D* value was considered proportional to the mean capillary segment length and average blood velocity (40). Nevertheless, clinical significance of D* values required further confirmation attributed to its low intrinsic signal-to-noise ratio (SNR) (32,41,42). However, no significant differences

 

were detected in ADC and D values between rectal cancers with and without LVI.

We found that rectal cancers at pN2 stages showed higher LVI rate than those at pN0 stages, which was consistent with previous studies. Brodsky *et al.* (43) reported that rectal cancers with LVI had a higher incidence of lymph node metastasis than those without LVI. Ishii *et al.* (44) found that lymph node metastasis was more frequently observed in LVI-positive rectal cancers. Chang *et al.* (45) revealed that LVI was one of the independent risk factors predicting lymph node metastasis in pT1-2 rectal carcinoma. In our study, we detected no significant correlations between LVI and other histopathological features, including maximum diameter, differentiation degree, pT, cM, and overall stage of rectal cancers. Okamoto *et al.* (46) also did not find any significant difference between LVI and the age, gender, size of tumor, location, differentiation degree in pT1-2 colorectal cancers. However, they revealed that LVI involved with hepatic metastasis rather than lymph node metastasis in that study. Sohn *et al.* (47) also reported that extramural vascular invasion was one of the risk factors for distant metastasis. Moreover, Du *et al.* (37) reported that LVI was significantly associated with histological differentiation and pTNM stage of rectal cancers. One reason for such discrepancies may be small patient population with distant metastasis (n=2) in our study, which needs more accumulation and further confirmation.

Colorectal cancers with LVI usually have a higher risk of disease progression, distant metastasis and poorer prognosis (2,3,48,49). For rectal cancers, LVI is also a crucial high-risk factor for recurrence after transanal endoscopic surgery (37). Therefore, it is important to identify rectal cancers with LVI before surgery. Kim *et al.* (50) reported that LVI of rectal cancers could be predicted preoperatively with a sensitivity of 68.2% and a specificity of 93.2% if a mesorectal perivascular infiltrative signal or vascular encasement by nodal tissues or signs of dirty mesorectal fat was observed on MR images. Smith *et al.* (51) demonstrated that extramural vascular invasion of rectal cancers could be predicted with a sensitivity of 62% and a specificity of 88% according to intermediate signal intensity apparent within vessels, or obvious irregular vessel contour or nodular expansion of vessel by definite tumor signal on MR images. Yet Sohn *et al.* (47) only reported a sensitivity of 28.2% with such criteria. Nevertheless, further ROC analysis in our study failed to detect significant diagnostic efficiency of f value in evaluating LVI status of rectal cancers, probably due to small sample size, which required further confirmation.

Another interesting finding of this study was that the IVIM derived ADC and D values showed no significant correlations with clinicopathological features, including maximum diameter, differentiation degree, pT, pN, cM, overall stage, LVI and neural invasion of rectal cancers. Akashi *et al.* (14) also reported no significant difference in mean ADCs when stratifying patients according to T-stage, N-stage, and presence of LVI. Curvo-Semedo *et al.* (15) demonstrated no significant difference in mean ADCs between various T stages of rectal cancers. Sun *et al.* (16) revealed no significant difference in mean ADCs among different histological grade, pN and neural invasion of rectal cancers. All the above findings might indicate distinct microstructural features of rectal cancers different from other gastroenterological tumors. For instance, Liu *et al.* (52,53) reported that both mean and minimum ADC values of the gastric cancers correlated with the postoperative T staging, N staging, TNM staging, histological differentiation and Lauren classification.

Our study had several limitations. First, the sample size was relatively small, yet was enough for a pilot study and a larger cohort should be enrolled in our future work. Second, we draw ROIs of tumor lesions manually without rigorous reference with postoperative specimens due to technique difficulty. Third, the number and distribution of b values were not optimized in IVIM sequence for rectal cancers. In our study, a total of 12 b values between 0 and 1,200 s/mm$^2$, 3 b values between 0 and 50 s/mm$^2$ and 5 b values between 0 and 100 s/mm$^2$ were used for IVIM parameters quantification in rectal cancers, which were more than multiple previous studies (30,54-56). We will use more low b values, especially between b=0 and b=50 s/mm$^2$ for IVIM parameters quantification in our future study.

## Conclusions

In conclusion, the current study demonstrated that the f and D* values of rectal cancers with LVI were significantly higher than those without LVI. Meanwhile, LVI rate differed significantly among rectal cancers at different pN stages. This pilot study indicated that the f value derived from IVIM imaging might hold a potential to predict LVI status of rectal carcinomas preoperatively, which required further confirmation in a larger cohort in future work.

## Acknowledgments

*Funding:* This work was supported by the National Health

 

and Family Planning Commission of China [W201306]; National Natural Science Foundation of China [81371516, 81601463]; Natural Science Foundation of Jiangsu Province [BK20150109]; Research Project of Health and Family Planning Commission of Jiangsu Province [Q201508]; Key Project supported by Medical Science and technology development Foundation, Nanjing Department of Health [YKK15067]; and Six Talent Peaks Project of Jiangsu Province [2015-WSN-079].

## Footnote

*Provenance and Peer Review:* This article was commissioned by the Guest Editors (Yì-Xiáng J. Wáng, Yong Wang) for the series "Translational Imaging in Cancer Patient Care" published in *Translational Cancer Research*. The article has undergone external peer review.

*Conflicts of Interest:* All authors have completed the ICMJE uniform disclosure form (available at http://dx.doi.org/10.21037/tcr.2017.08.23). The series "Translational Imaging in Cancer Patient Care" was commissioned by the editorial office without any funding or sponsorship. The authors have no other conflicts of interest to declare.

*Ethical Statement:* The authors are accountable for all aspects of the work in ensuring that questions related to the accuracy or integrity of any part of the work are appropriately investigated and resolved. The study was conducted in accordance with the Declaration of Helsinki (as revised in 2013). This prospective study was approved by the local ethics committee at our hospital (No.2014-027-02) and written informed consents were obtained from all the patients.



## References

1. Wang Y, Li L, Wang YX, et al. Time-intensity curve parameters in rectal cancer measured using endorectal ultrasonography with sterile coupling gels filling the rectum: correlations with tumor angiogenesis and clinicopathological features. Biomed Res Int 2014;2014:587806.
2. Ross A, Rusnak C, Weinerman B, et al. Recurrence and survival after surgical management of rectal cancer. Am J Surg 1999;177:392-5.
3. Compton CC, Fielding LP, Burgart LJ, et al. Prognostic factors in colorectal cancer. College of American Pathologists Consensus Statement 1999. Arch Pathol Lab Med 2000;124:979-94.
4. Cui NY, Liu JY, Wang Y, et al. Contrast enhanced ultrasound guided biopsy shows higher positive sampling rate than conventional ultrasound guided biopsy for gastrointestinal stromal tumors diagnosis. Transl Cancer Res 2016;5:152-9.
5. Bettoni F, Masotti C, Habr-Gama A, et al. Intratumoral Genetic Heterogeneity in Rectal Cancer: Are Single Biopsies representative of the entirety of the tumor? Ann Surg 2017;265:e4-6.
6. Rao SX, Zeng MS, Xu JM, et al. Assessment of T staging and mesorectal fascia status using high-resolution MRI in rectal cancer with rectal distention. World J Gastroenterol 2007;13:4141-6.
7. Giusti S, Buccianti P, Castagna M, et al. Preoperative rectal cancer staging with phased-array MR. Radiat Oncol 2012;7:29.
8. Ucar A, Obuz F, Sokmen S, et al. Efficacy of high resolution magnetic resonance imaging in preoperative local staging of rectal cancer. Mol Imaging Radionucl Ther 2013;22:42-8.
9. Jhaveri KS, Hosseini-Nik H. MRI of rectal cancer: an overview and update on recent advances. AJR Am J Roentgenol 2015;205:W42-55.
10. Lu ZH, Hu CH, Qian WX, et al. Preoperative diffusion-weighted imaging value of rectal cancer: preoperative T staging and correlations with histological T stage. Clin Imaging 2016;40:563-8.
11. Kim SH, Yoon JH, Lee Y. Added value of morphologic characteristics on diffusion-weighted images for characterizing lymph nodes in primary rectal cancer. Clin Imaging 2015;39:1046-51.
12. Mannelli L, Nougaret S, Vargas HA, et al. Advances in Diffusion-Weighted Imaging. Radiol Clin North Am 2015;53:569-81.
13. Eghtedari M, Ma J, Fox P, et al. Effects of magnetic field strength and b value on the sensitivity and specificity

 

of quantitative breast diffusion-weighted MRI. Quant Imaging Med Surg 2016;6:374-80.
14. Akashi M, Nakahusa Y, Yakabe T, et al. Assessment of aggressiveness of rectal cancer using 3-T MRI: correlation between the apparent diffusion coefficient as a potential imaging biomarker and histologic prognostic factors. Acta Radiol 2014;55:524-31.
15. Curvo-Semedo L, Lambregts DM, Maas M, et al. Diffusion-Weighted MRI in Rectal Cancer: Apparent Diffusion Coefficient as a Potential Noninvasive Marker of Tumor Aggressiveness. J Magn Reson Imaging 2012;35:1365-71.
16. Sun Y, Tong T, Cai S, et al. Apparent diffusion coefficient (ADC) value: a potential imaging biomarker that reflects the biological features of rectal cancer. PloS One 2014;9:e109371.
17. Mazaheri Y, Afaq A, Rowe DB, et al. Diffusion weighted magnetic resonance imaging of the prostate: improved robustness with stretched exponential modeling. J Comput Assist Tomogr 2012;36:695-703.
18. Le Bihan D, Turner R. The capillary network: a link between IVIM and classical perfusion. Magn Reson Med 1992;27:171-8.
19. Le Bihan D, Breton E, Lallemand D, et al. Separation of diffusion and perfusion in intravoxel incoherent motion MR imaging. Radiology 1988;168:497-505.
20. Wáng YXJ, Deng M, Li YT, et al. A combined use of intravoxel incoherent motion MRI parameters can differentiate early stage hepatitis-b fibrotic livers from healthy livers. SLAS Technol 2017. [Epub ahead of print].
21. Zhang Q, King AD, Bhatia KS, et al. Improving intra-voxel incoherent motion MRI quantification using wild bootstrap. IEEE 11th International Symposium on Biomedical Imaging (ISBI) 2014:726-9.
22. Li YT, Cercueil JP, Yuan J, et al. Liver intravoxel incoherent motion (IVIM) magnetic resonance imaging: a comprehensive review of published data on normal values and applications for fibrosis and tumor evaluation. Quant Imaging Med Surg 2017;7:59-78.
23. Lu PX, Huang H, Yuan J, et al. Decreases in molecular diffusion, perfusion fraction and perfusion-related diffusion in fibrotic livers: a prospective clinical intravoxel incoherent motion MR imaging study. PLoS One 2014;9:e113846.
24. Yuan J, Wong OL, Lo GG, et al. Statistical assessment of bi-exponential diffusion weighted imaging signal characteristics induced by intravoxel incoherent motion in malignant breast tumors. Quant Imaging Med Surg 2016;6:418-29.
25. Klau M, Mayer P, Bergmann F, et al. Correlation of histological vessel characteristics and diffusion-weighted imaging intravoxel incoherent motion-derived parameters in pancreatic ductal adenocarcinomas and pancreatic neuroendocrine tumors. Invest Radiol 2015;50:792-7.
26. Rheinheimer S, Stieltjes B, Schneider F, et al. Investigation of renal lesions by diffusion-weighted magnetic resonance imaging applying intravoxel incoherent motion-derived parameters--initial experience. Eur J Radiol 2012;81:e310-6.
27. Yang DM, Kim HC, Kim SW, et al. Prostate cancer: correlation of intravoxel incoherent motion MR parameters with Gleason score. Clin Imaging 2016;40:445-50.
28. Zhang YD, Wang Q, Wu CJ, et al. The histogram analysis of diffusion-weighted intravoxel incoherent motion (IVIM) imaging for differentiating the gleason grade of prostate cancer. Eur Radiol 2015;25:994-1004.
29. Nougaret S, Vargas HA, Lakhman Y, et al. Intravoxel Incoherent Motion-derived Histogram Metrics for Assessment of Response after Combined Chemotherapy and Radiation Therapy in Rectal Cancer: Initial Experience and Comparison between Single-Section and Volumetric Analyses. Radiology 2016;280:446-54.
30. Bäuerle T, Seyler L, Münter M, et al. Diffusion-weighted imaging in rectal carcinoma patients without and after chemoradiotherapy: a comparative study with histology. Eur J Radiol 2013;82:444-52.
31. Yu XP, Wen L, Hou J, et al. Discrimination between metastatic and nonmetastatic mesorectal lymph nodes in rectal cancer using intravoxel incoherent motion diffusion-weighted magnetic resonance imaging. Acad Radiol 2016;23:479-85.
32. Qiu L, Liu XL, Liu SR et al. Role of quantitative intravoxel incoherent motion parameters in the preoperative diagnosis of nodal metastasis in patients with rectal carcinoma. J Magn Reson Imaging 2016;44:1031-9.
33. Marquardt D. An algorithm for least-squares estimation of nonlinear parameters. J Soc Indust Appl Math 1963;11:431-41.
34. Lemke A, Laun FB, Simon D, et al. An in vivo verification of the intravoxel incoherent motion effect in diffusion-weighted imaging of the abdomen. Magn Reson Med 2010;64:1580-5.
35. Sun H, Xu Y, Xu Q, et al. Rectal cancer: Short-term reproducibility of intravoxel incoherent motion parameters in 3.0T magnetic resonance imaging. Medicine (Baltimore) 2017;96:e6866.
36. Chiaradia M, Baranes L, Van Nhieu JT, et al. Intravoxel

 

incoherent motion (IVIM) MR imaging of colorectal liver metastases: are we only looking at tumor necrosis? J Magn Reson Imaging 2014;39:317-25.
37. Du CZ, Xue WC, Cai Y, et al. Lymphovascular invasion in rectal cancer following neoadjuvant radiotherapy: A retrospective cohort study. World J Gastroenterol 2009;15:3793-8.
38. Wu CC, Lee RC, Chang CY. Prediction of lymphovascular invasion in rectal cancer by preoperative CT. AJR Am J Roentgenol 2013;201:985-92.
39. Yao WW, Zhang H, Ding B, et al. Rectal cancer: 3D dynamic contrast-enhanced MRI; correlation with microvascular density and clinicopathological features. Radiol Med 2011;116:366-74.
40. Le Bihan D, Breton E, Lallemand D, et al. MR imaging of intravoxel incoherent motions: application to diffusion and perfusion in neurologic disorders. Radiology 1986;161:401-7.
41. Liu C, Wang K, Chan Q, et al. Intravoxel incoherent motion MR imaging for breast lesions: comparison and correlation with pharmacokinetic evaluation from dynamic contrast-enhanced MR imaging. Eur Radiol 2016;26:3888-98.
42. Zhang Q, Wang YX, Ma HT, et al. Cramer-Rao bound for intravoxel incoherent motion diffusion weighted imaging fitting. Conf Proc IEEE Eng Med Biol Soc 2013;2013:511-4.
43. Brodsky JT, Richard GK, Cohen AM, et al. Variables correlated with the risk of lymph node metastasis in early rectal cancer. Cancer 1992;69:322-6.
44. Ishii M, Ota M, Saito S, et al. Lymphatic vessel invasion detected by monoclonal antibody D2-40 as a predictor of lymph node metastasis in T1 colorectal cancer. Int J Colorectal Dis 2009;24:1069-74.
45. Chang HC, Huang SC, Chen JS, et al. Risk factors for lymph node metastasis in pt1 and pt2 rectal cancer: a single-institute experience in 943 patients and literature review. Ann Surg Oncol 2012;19:2477-84.
46. Okamoto Y, Mitomi H, Ichikawa K, et al. Effect of skip lymphovascular invasion on hepatic metastasis in colorectal carcinomas. Int J Clin Oncol 2015;20:761-6.
47. Sohn B, Lim JS, Kim H, et al. MRI-detected extramural vascular invasion is an independent prognostic factor for synchronous metastasis in patients with rectal cancer. Eur Radiol 2015;25:1347-55.
48. Koukourakis MI, Giatromanolaki A, Sivridis E, et al. Inclusion of vasculature -related variables in the Dukes staging system of colon cancer. Clin Cancer Res 2005;11:8653-60.
49. Goossens N, Nakagawa S, Sun X, et al. Cancer biomarker discovery and validation. Transl Cancer Res 2015;4:256-69.
50. Kim Y, Chung JJ, Yu JS, et al. Preoperative evaluation of lymphovascular invasion using high-resolution pelvic magnetic resonance in patients with rectal cancer: a 2-year follow-up study. J Comput Assist Tomogr 2013;37:583-8.
51. Smith NJ, Barbachano Y, Norman AR, et al. Prognostic significance of magnetic resonance imaging detected extramural vascular invasion in rectal cancer. Br J Surg 2008;95:229-36.
52. Liu S, Wang H, Guan W, et al. Preoperative apparent diffusion coefficient value of gastric cancer by diffusion-weighted imaging: correlations with postoperative TNM Staging. J Magn Reson Imaging 2015;42:837-43.
53. Liu S, Guan W, Wang H, et al. Apparent diffusion coefficient value of gastric cancer by diffusion-weighted imaging: correlations with the histological differentiation and Lauren classification. Eur J Radiol 2014;83:2122-8.
54. Surov A, Meyer HJ, Höhn AK, et al. Correlations between intravoxel incoherent motion (IVIM) parameters and histological findings in rectal cancer: preliminary results. Oncotarget 2017;8:21974-83.
55. Fusco R, Sansone M, Petrillo A. A comparison of fitting algorithms for diffusion-weighted MRI data analysis using an intravoxel incoherent motion model. MAGMA 2017;30:113-20.
56. Ganten MK, Schuessler M, Bäuerle T, et al. The role of perfusion effects in monitoring of chemoradiotherapy of rectal carcinoma using diffusion-weighted imaging. Cancer Imaging 2013;13:548-56.

**Cite this article as:** Yan C, Pan X, Chen G, Ge W, Liu S, Li M, Nie L, He J, Zhou Z. A pilot study on correlations between preoperative intravoxel incoherent motion MR imaging and postoperative histopathological features of rectal cancers. Transl Cancer Res 2017;6(6):1050-1060. doi: 10.21037/tcr.2017.08.23

 